https://ntrs.nasa.gov/search.jsp?R=20170006857 2019-08-31T06:40:47+00:00Z

High Temperature Degradation of Advanced Thermal and Environmental Barrier Coatings (TEBCs) by CaO-MgO-Al2O3-SiO2 (CMAS)

GUSTAVO COSTA AND DONGMING ZHU

Environmental Effects and Coatings Branch
Materials and Structures Division
NASA Glenn Research Center, Cleveland, OH 44135
gustavo.costa@nasa.gov

12th Pacific Rim Conference on Ceramic and Glass Technology (PACRIM 12)

Outline of Presentation

- Thermal and Environmental Barrier Coating Systems
- Experimental
  - Sample preparation and reaction with CMAS
- Results
  - Thermodynamic modeling of YSZ-CMAS system
  - Characterization:

1 - Pristine NASA composition CMAS by XRD, ICP-OAS and DSC

2 - CMAS reacted with the hollow tube coating specimens by SEM-EDS and XRD

- Summary

Thermal and Environment Barrier Coating Developments

Baseline ZrO_2-(7-8)wt%Y_2O_3 and Rare Earth Doped-Low Conductivity Thermal Barrier Coating Systems - Continued

Baseline ZrO_2-(7-8) wt%Y_2O_3:

- Relatively low intrinsic thermal conductivity ~2.5 W/m-K
- High thermal expansion to better match superalloy substrates
- Good high temperature stability and mechanical properties
- Additional conductivity reduction by micro-porosity

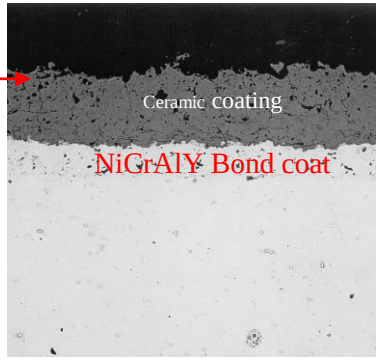

Low Conductivity Defect Cluster Thermal Barrier Coatings

— Multi-component oxide defect clustering approach

e.g.: ZrO_2/HfO_2-Y_2O_3-Nd_2O_3(Gd_2O_3,Sm_2O_3)-Yb_2O_3(Sc_2O_3) systems

Primary stabilizer

Oxide cluster dopants with distinctive ionic sizes

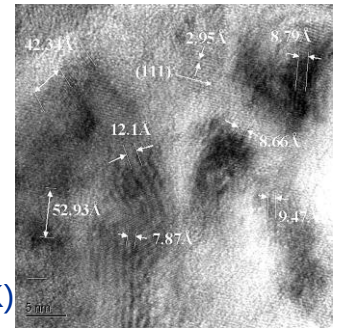

Plasma-sprayed ZrO_2-(Y, Nd,Yb)$_2O_3$

— Defect clusters associated with dopant segregation

— The 5 to 100 nm size defect clusters for significantly reduced thermal conductivity (0.5-1.2 W/m-K) and improved stability

— Advanced TEBC systems for Ceramic Matrix Composites use the low k based compositions

TEBCs-CMAS Degradation is of Concern with Increasing Operating Temperatures

Experimental:sample preparation and heat treatment

- Air plasma sprayed coating (0.030” thickness) specimens on to 1/8” diameter graphite bar substrates then 1500 °C, 5 h sintering, resulting hollow tubes.
- NASA composition CMAS used for reaction at 1300 ° C for 5h.

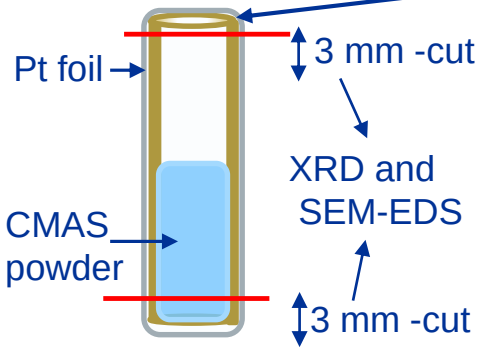

	Hollow Tube composition mole (%)	ρ (%) *	Average pore vol. (mm^3) **
cubic	ZrO_2-12Y_2O_3	90(3)	35(2)
	ZrO_2- 30Y_2O_3	81(3)	-
	HfO_2-7Dy_2O_3	89(3)	21(3)
	ZrO_2- 9Y_2O_3- 4.5Gd_2O_3- 4.5Yb_2O_3	100 (3)	3(7)
	ZrO_2- 9.6Y_2O_3- 2.2Gd_2O_3- 2.1Yb_2O_3	90(3)	23(4)
tetragonal	ZrO_2- 3Y_2O_3- 1.5Nd_2O_3- 1.5Yb_2O_3- 0.3Sc_2O_3	90(3)	20(3)
	ZrO_2- 3Y_2O_3-1.5Sm_2O_3-1.5Yb_2O_3	98(3)	4(3)

*(ρgeometric*100/ρHe). **ρgeometric-ρHe.

(1:10 CMAS to sample mass ratio, concentration of 70-150 mg/cm^2)

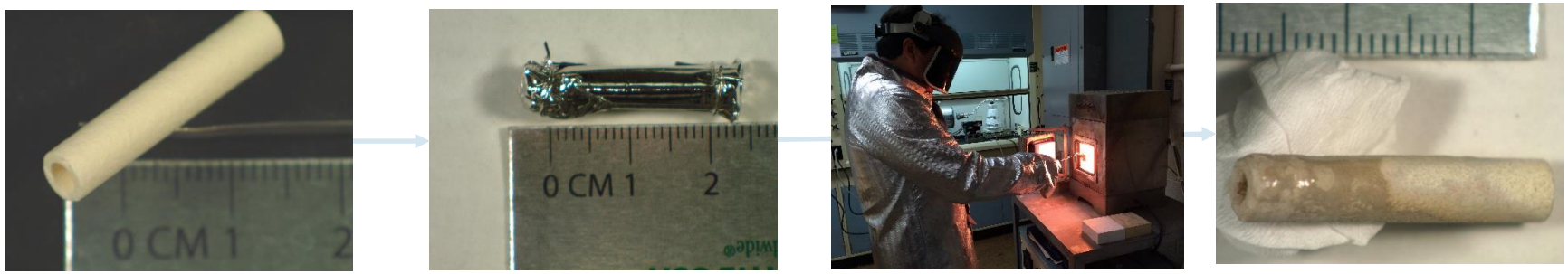

(A) (B) (C)

Hollow 12YSZ tube samples: (A) pristine; (B) before heat treatment in which it was half filled with CMAS powder, wrapped and sealed with Pt foil; (C) after heat treatment at 1310 °C for 30 min and unwrapped.

Results: characterization of NASA composition CMAS (as processed) before reaction

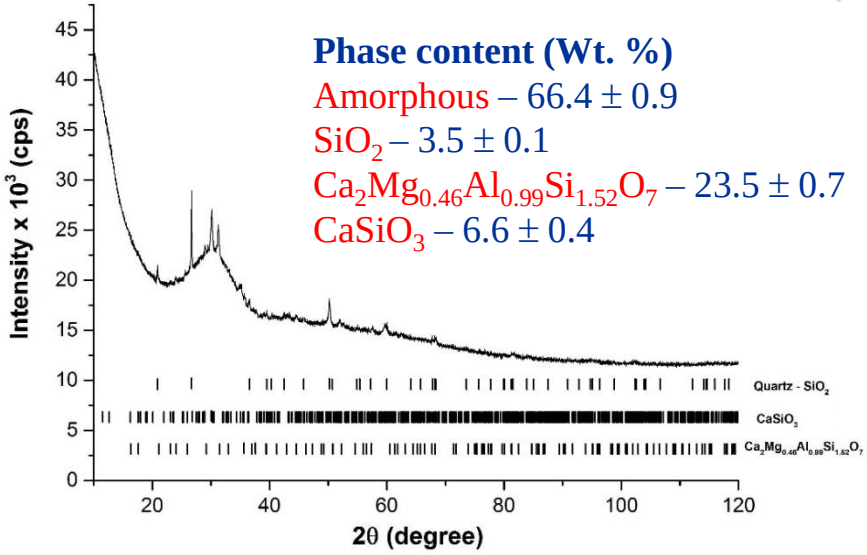

Phase content (Wt. %)

Amorphous – 66.4 ± 0.9

SiO_2 – 3.5 ± 0.1

$Ca_2Mg_{0.46}Al_{0.99}Si_{1.52}O_7$ – 23.5 ± 0.7

$CaSiO_3$ – 6.6 ± 0.4

X-ray diffraction patterns of the as-received CMAS sample.

Chemical analysis of the as-received NASA CMAS by ICP-OAS

Element	Amount (wt. %)	±
Ca	21	1
Mg	3.1	0.2
Al	6.1	0.3
Si	19	1
Fe	5.9	0.3
Ni	1.10	0.06

Trace elements found but not quantified are
Ba, Cr, Cu, K, Mn, Na, Sr, Ti, Zr

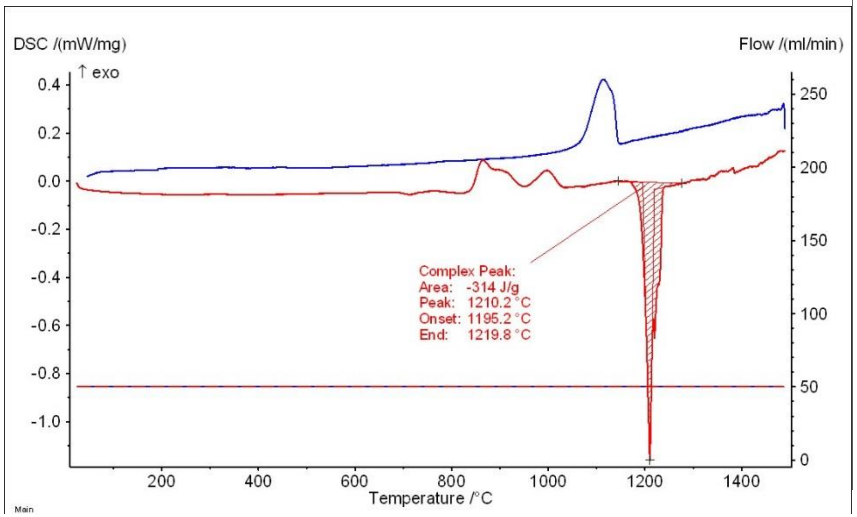

DSC traces of CMAS during heating and cooling up to 1500 °C at 5 °C/min.

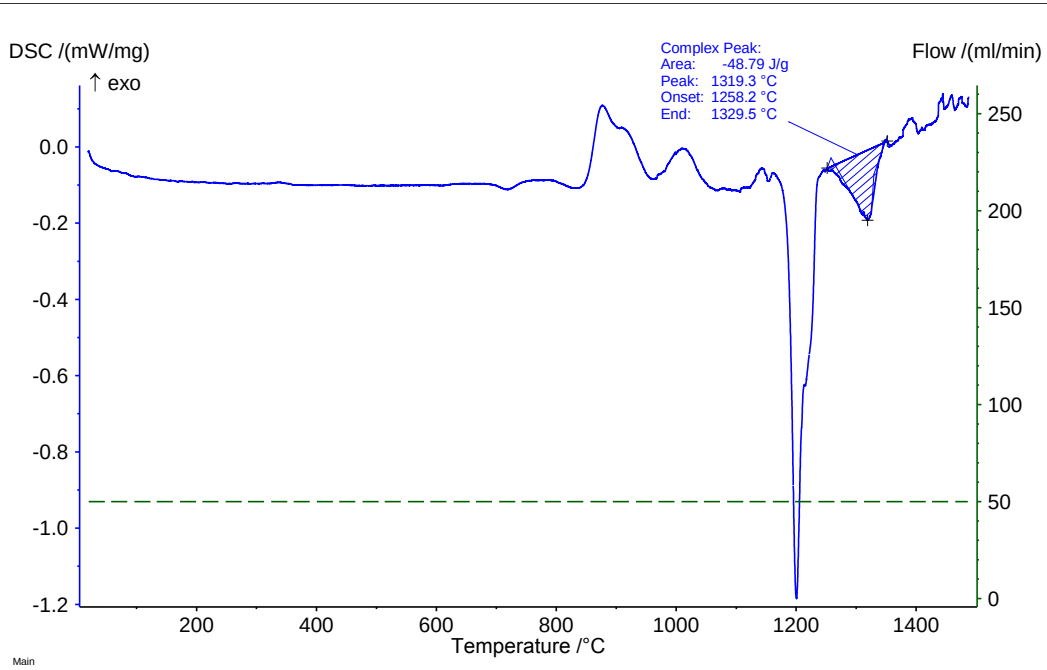

DSC traces of CMAS mixed with 18YSZ (1:2 mass ratio) during **heating** up to 1500 °C at 5 °C/min.

Results: Thermochemical modeling of YSZ – CMAS system using Thermocalc and TCOX6 database

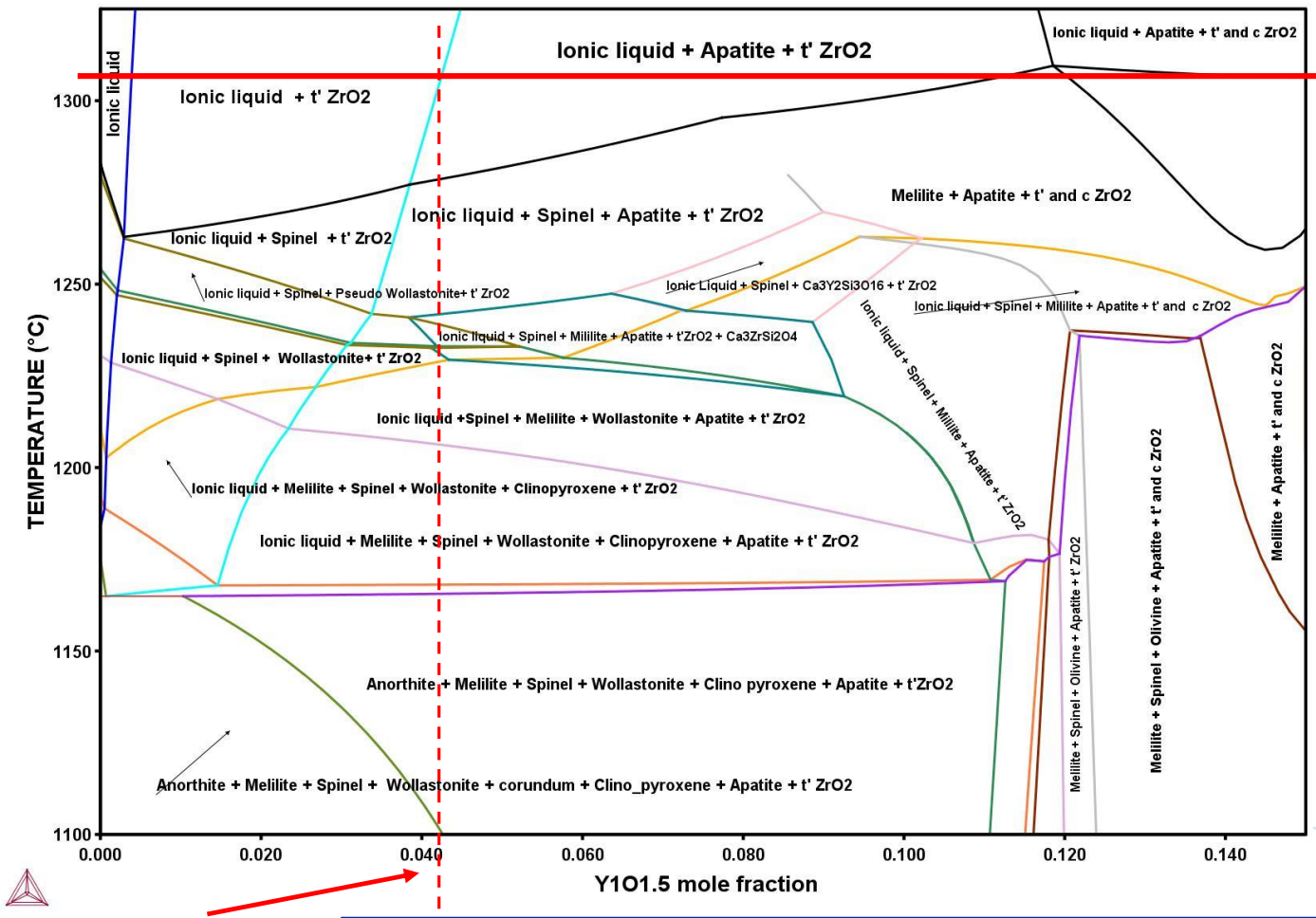

Reaction T of the experiments

Calculated phase diagram of CMS-YSZ system.

Input oxide amounts

Component	Mole
CaO	35
MgO	8
Al_2O_3	7
SiO_2	45
Fe_2O_3	3
NiO	1
ZrO_2	82
Y_2O_3	18

8 mol% Y_2O_3

2.3 mol% Y_2O_3
Baseline TBC

Output:
T - 1316.85 °C

Fluoride

Component	Mol
CaO	1.7e-2
MgO	2.5e-3
$FeO_{1.5}$	1.7e-7
$AlO_{1.5}$	1e-3
NiO	4.4e-3
SiO_2	3.0e-5
ZrO_2	8.9e-1
$Y_1O_{1.5}$	8.4e-2

ZrO_2_tetragonal

Component	Mol
CaO	8.1e-3
MgO	5.1e-5
$FeO_{1.5}$	8.6e-8
NiO	3.8e-3
ZrO_2	9.7e-1
$Y_1O_{1.5}$	1.8e-2

Apatite

Component	Mol
CaO	1.1e-1
MgO	2e-4
SiO_2	2.7e-1
$Y_1O_{1.5}$	6.2 e-1

Ionic_liq#2

Component	Mol
CaO	2.8e-1
MgO	9.3e-2
SiO_2	3.8e-1
$FeO_{1.5}$	9.3-1
NiO	2.2e-2
ZrO_2	2.7e-2

Results: SEM cross-section images at low magnification (lower cut section)

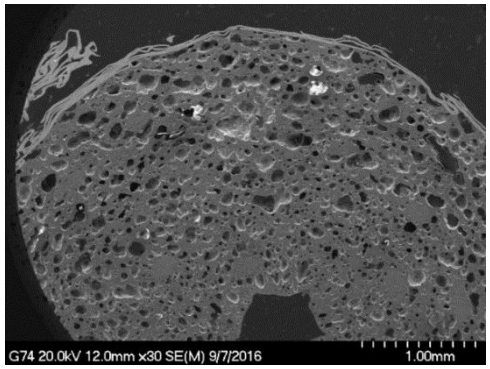

12YSZ

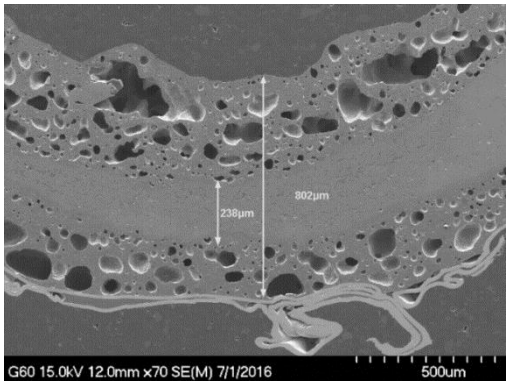

30YSZ

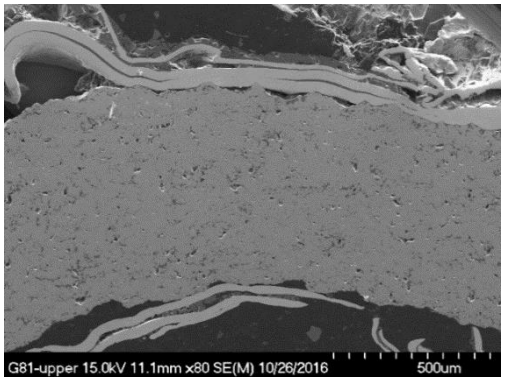

7DySH

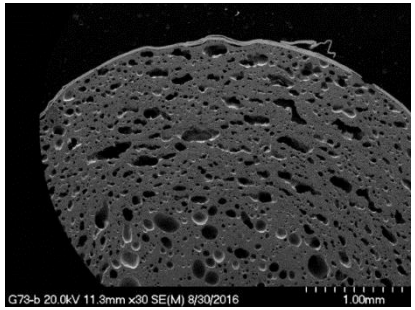

ZrO_2-9.0Y_2O_3-4.5Gd_2O_3-4.5Yb_2O_3

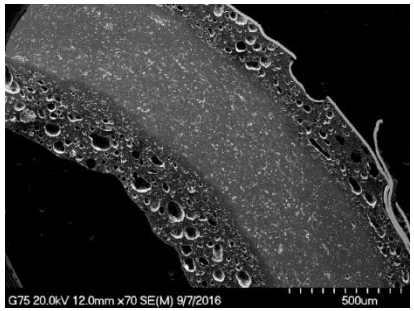

ZrO_2-9.6Y_2O_3-2.2Gd_2O_3-2.1Yb_2O_3

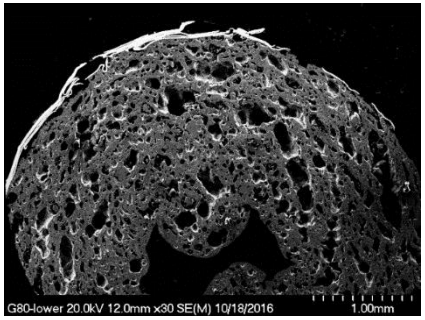

ZrO_2-3.0Y_2O_3-1.5Sm_2O_3-1.5Yb_2O_3

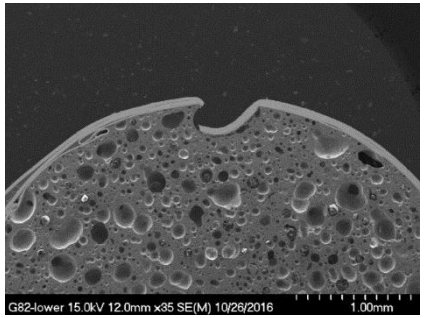

ZrO_2-3.0Y_2O_3-1.5Nd_2O_3-1.5Yb_2O_3-0.3Sc_2O_3

SEM cross – sectional electron images of the lower section of the ceramic hollow tube samples reacted with CMAS at 1300 °C for 5 h.

Results: 12YSZ lower section of the hollow tube reacted with CMAS.

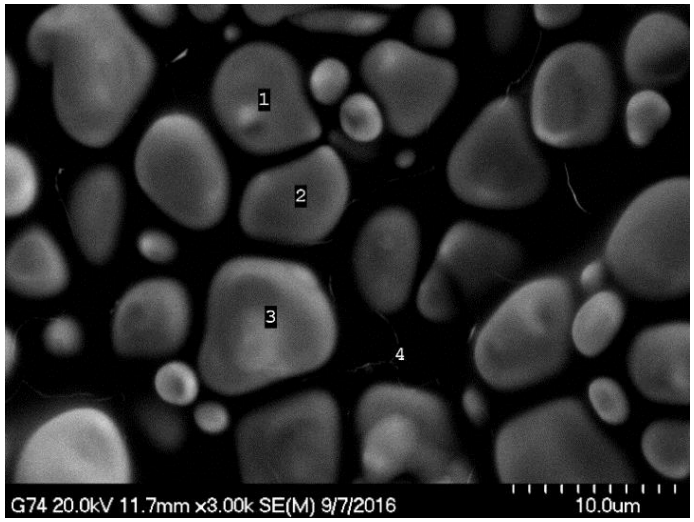

SEM image of (reacted region) at high magnification.

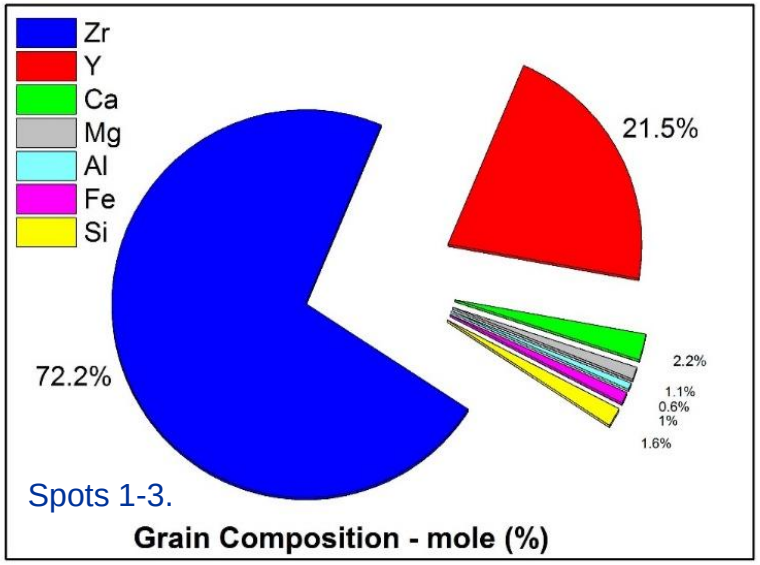

Spots 1-3.

Grains 1-3	ZrO_2	Y_2O_3
Nominal mole (%)	88	12
EDS mole (%)	81 (1)	11.9(2)

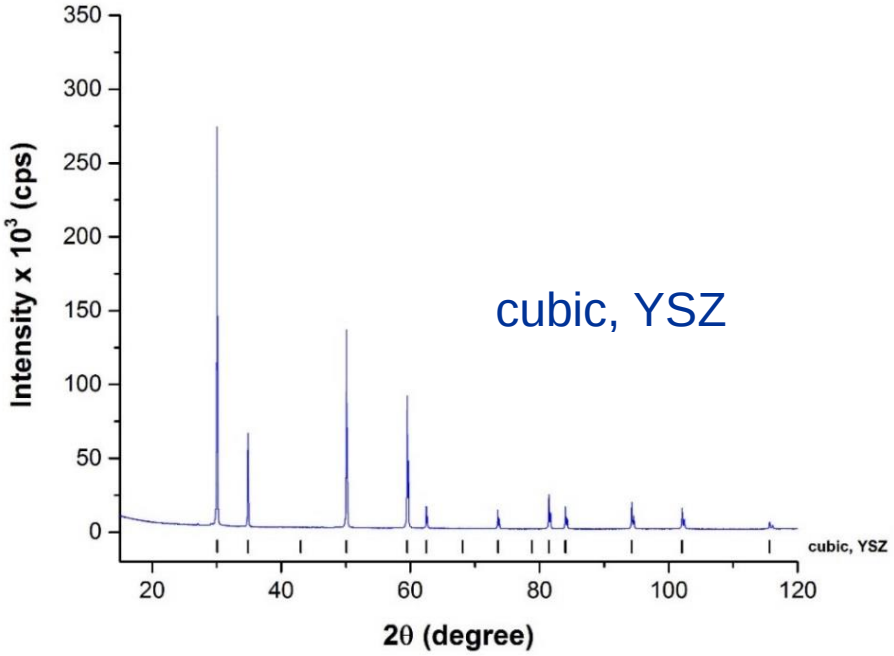

XRD pattern of the ground hollow tube.

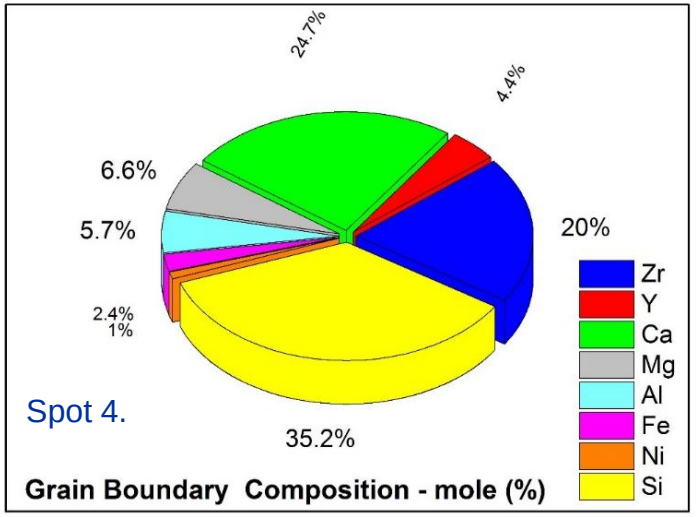

Spot 4.

Elemental content from EDS.

Results: 30YSZ lower section of the hollow tube reacted with CMAS.

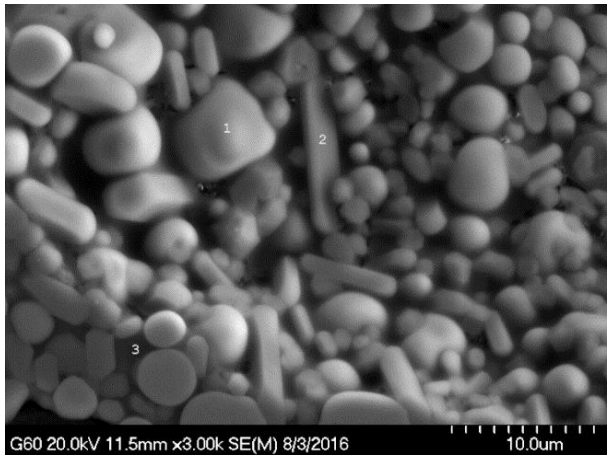

SEM image at high magnification.

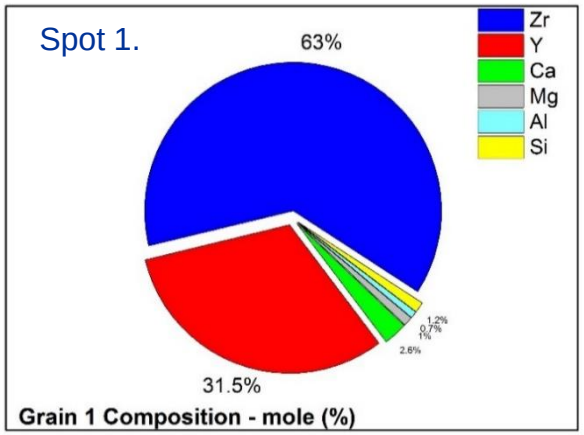

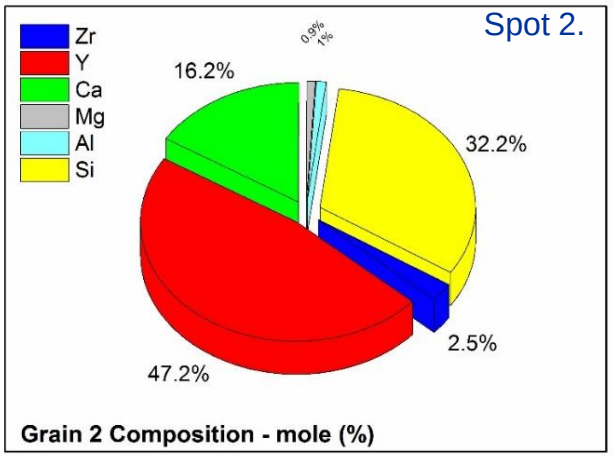

Grain 1	ZrO_2	Y_2O_3
Nominal mole (%)	81	18
EDS mole (%)	75(2)	19(1)

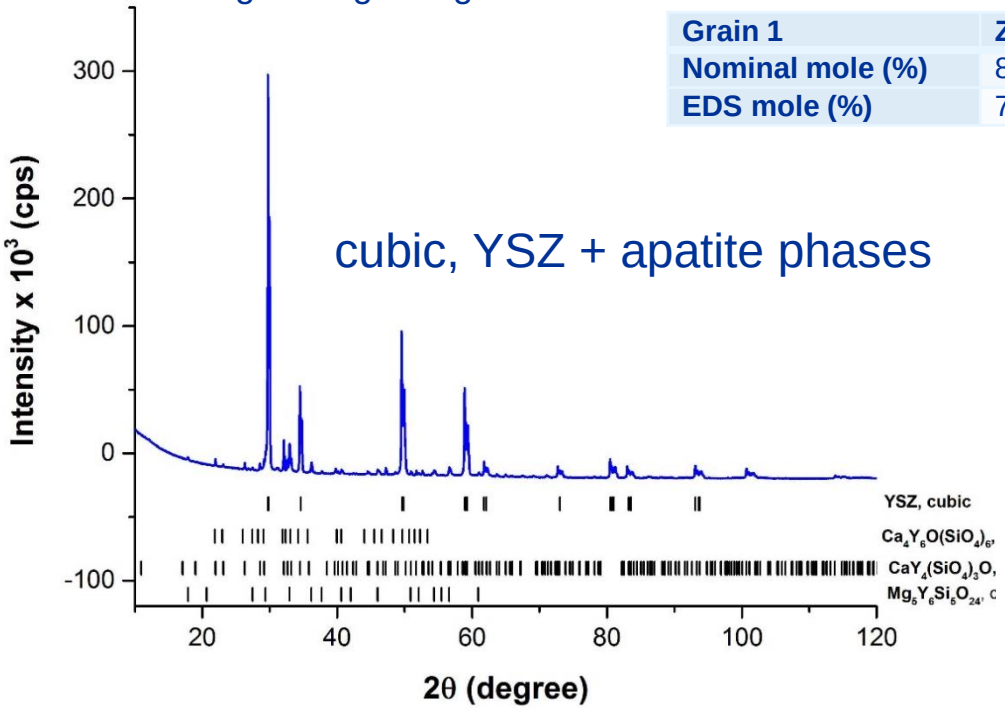

X-ray diffraction of the ground hollow tube.

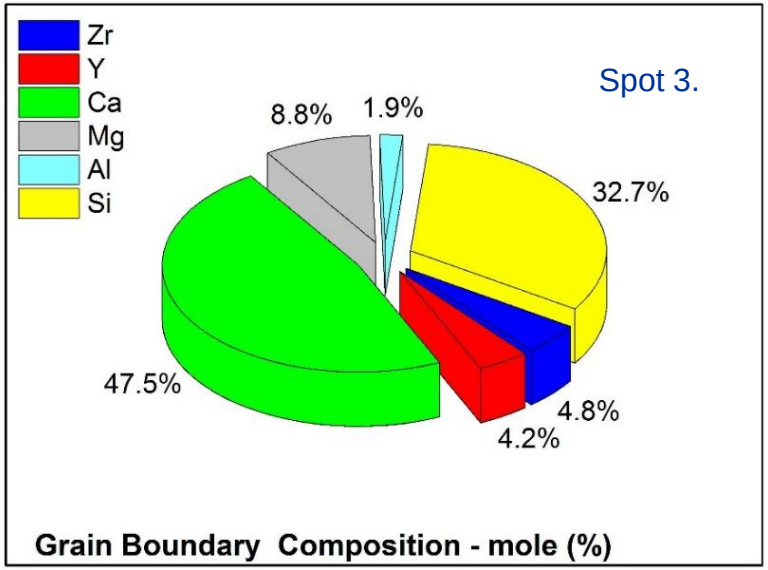

Elemental content from EDS.

Results: 7DySH lower section of the hollow tube reacted with CMAS.

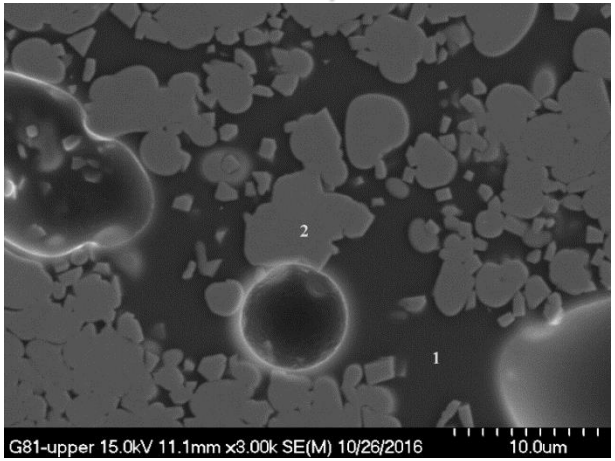

SEM image at high magnification.

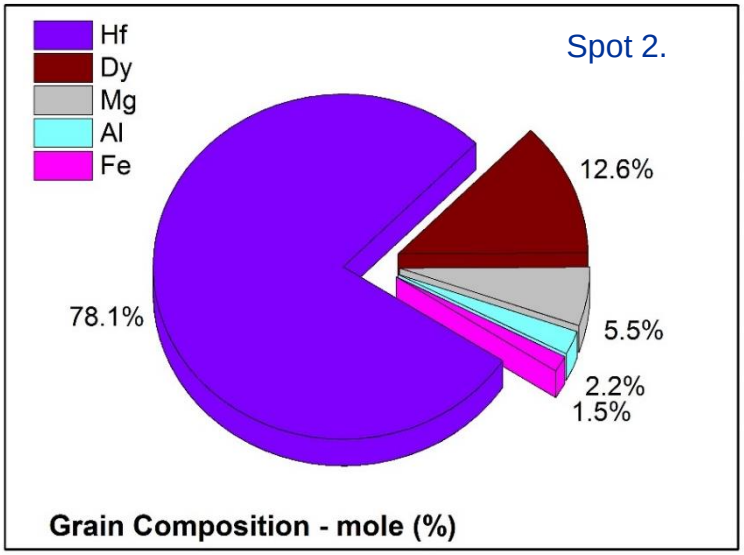

Grain 2	HfO_2	Dy_2O_3
Nominal mole (%)	93	7
EDS mole (%)	85(5)	7(1)

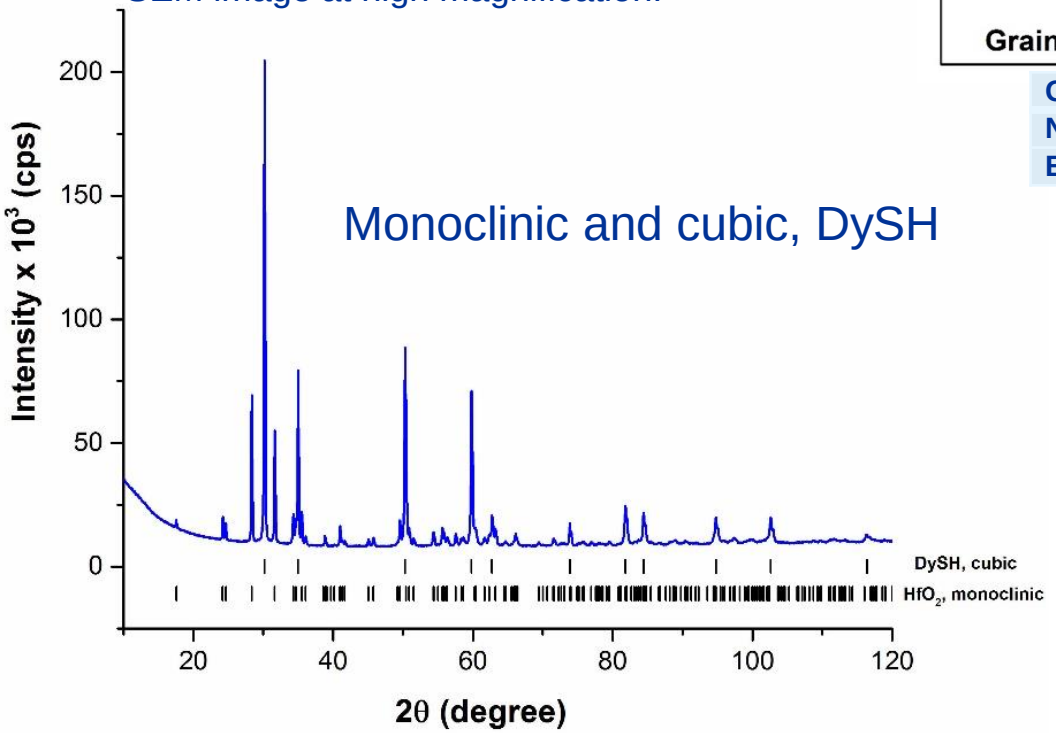

Monoclinic and cubic, DySH

XRD pattern of the ground hollow tube.

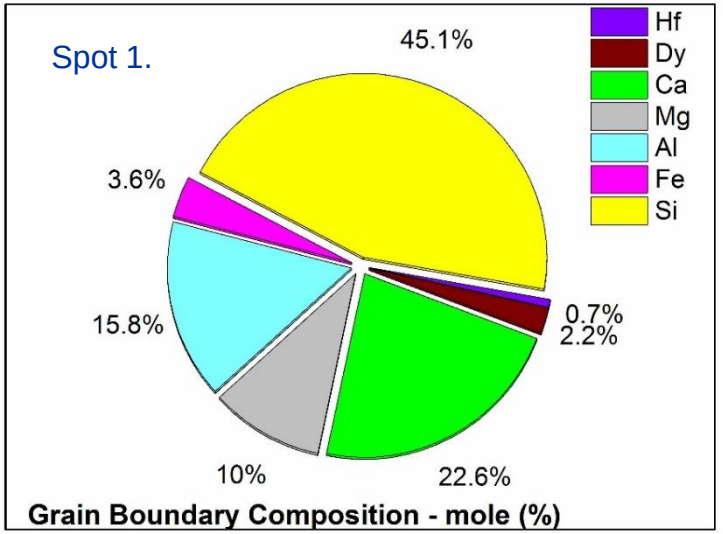

Elemental content from EDS.

Results Rare Earth Content *versus* apatite phase formation.

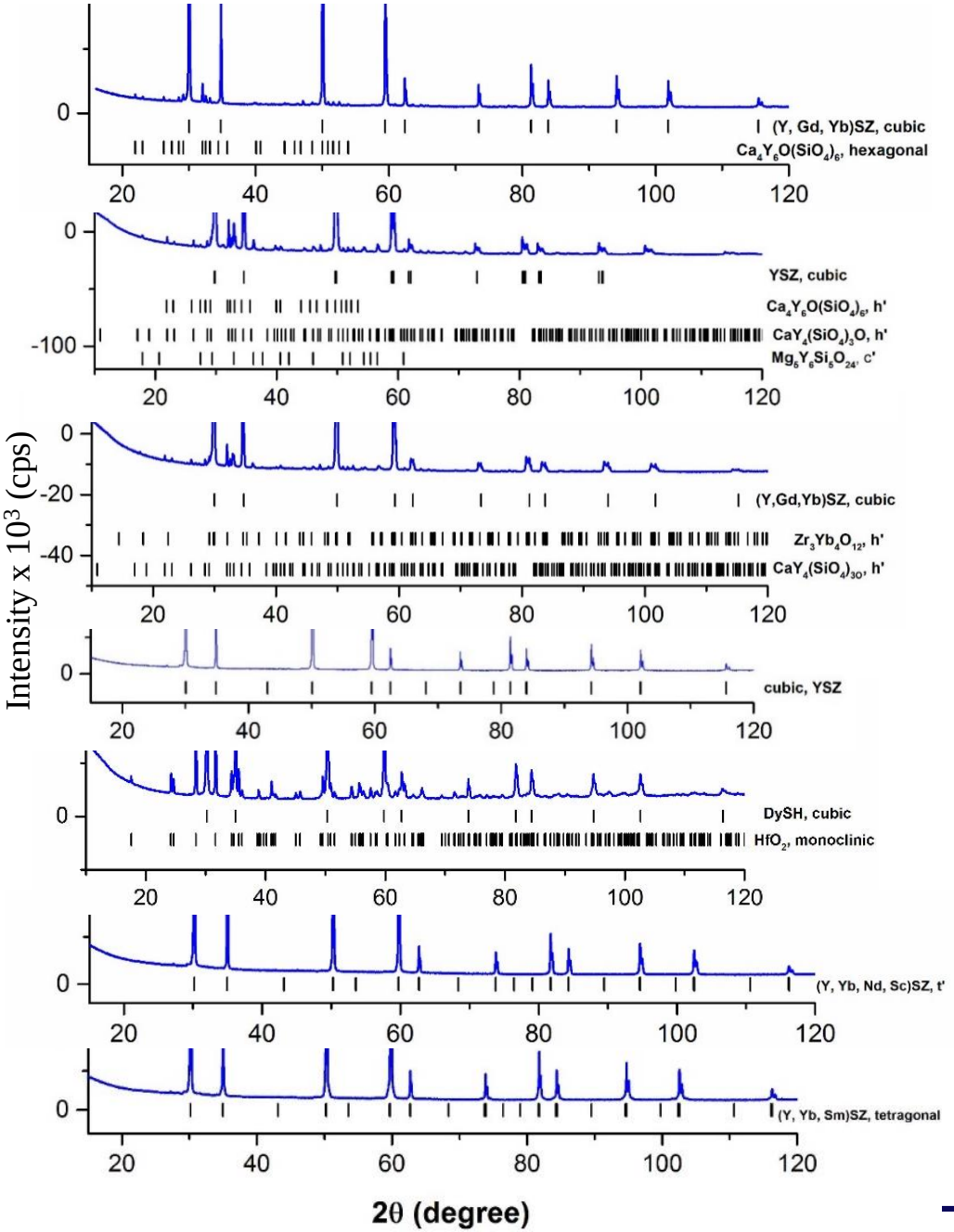

ZrO_2-18RE_2O_3 (RE = Y, Gd and Yb)

ZrO_2-30Y_2O_3

ZrO_2-13.9RE_2O_3 (RE = Y, Gd and Yb)

ZrO_2-12Y_2O_3

HfO_2-6.3Dy_2O_3

ZrO_2-6.3RE_2O_3 (RE = Y, Nd, Yb and Sc)

ZrO_2-6.0RE_2O_3 (RE = Y, Sm and Yb)

XRD patterns of the ground hollow tubes reacted with CMAS at 1310 °C for 5 h (lower cut section).

Results: content of the Rare-earth in the glass/silicate phase.

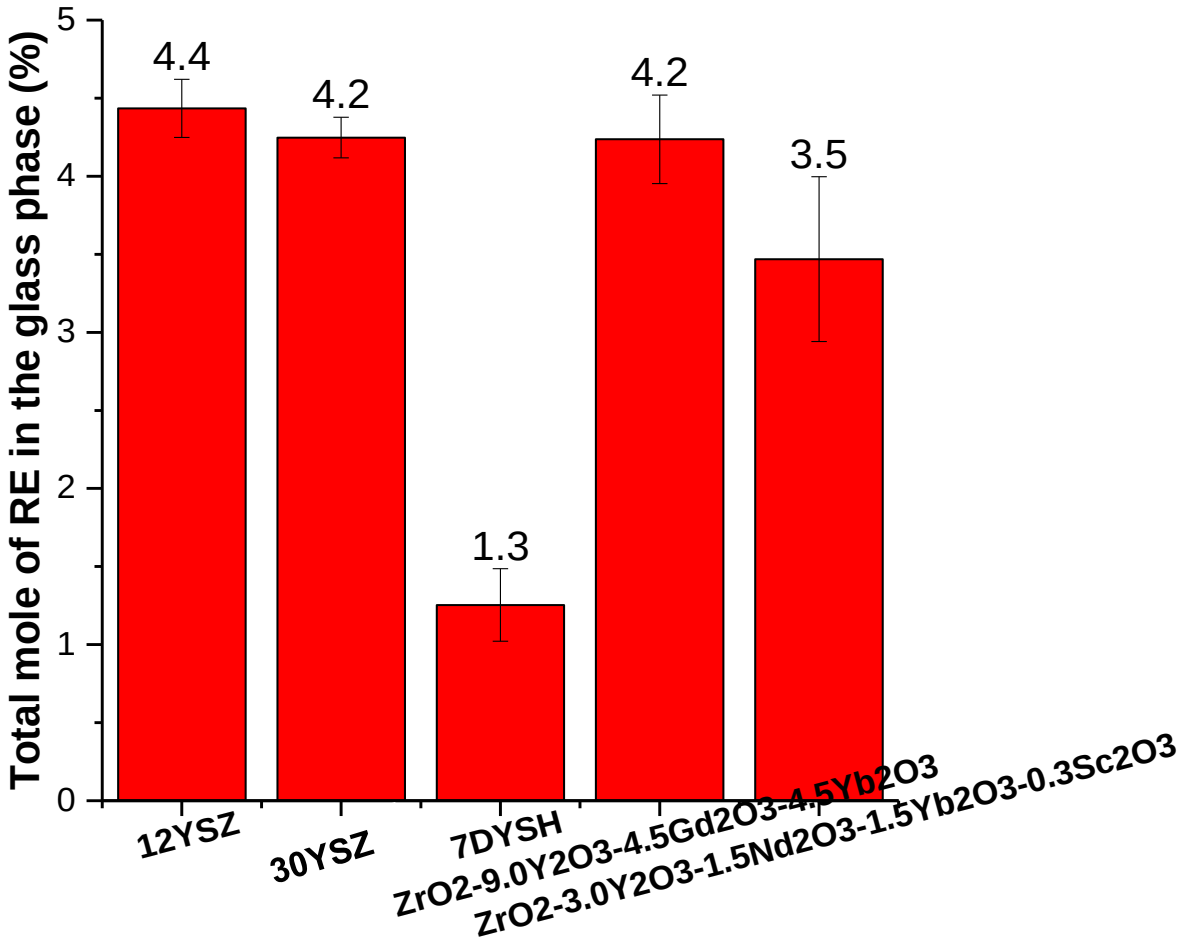

Depedence of the Rare-earth content in the glass/silicate phase versus Rare-earth content in the coating.

Results: content of the Rare-earth in the glass/silicate phase.

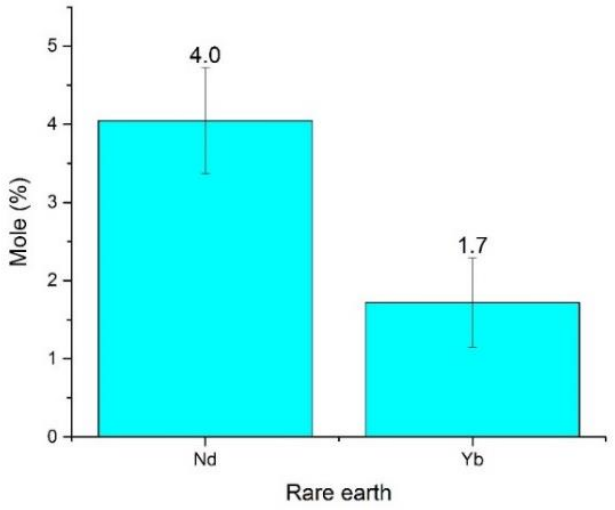

ZrO_2-3.0Y_2O_3-1.5Nd_2O_3-1.5Yb_2O_3-0.3Sc_2O_3

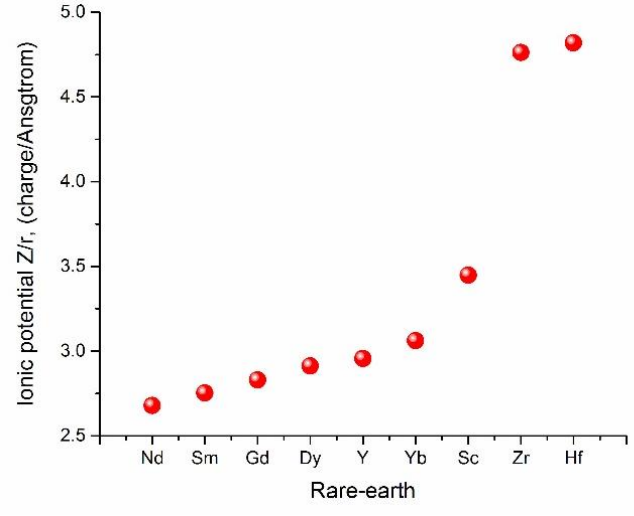

Ionic potential trend of RE

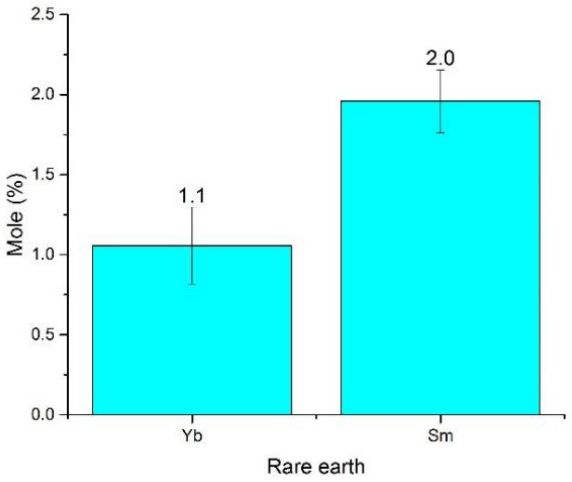

ZrO_2-3.0Y_2O_3-1.5Sm_2O_3-1.5Yb_2O_3

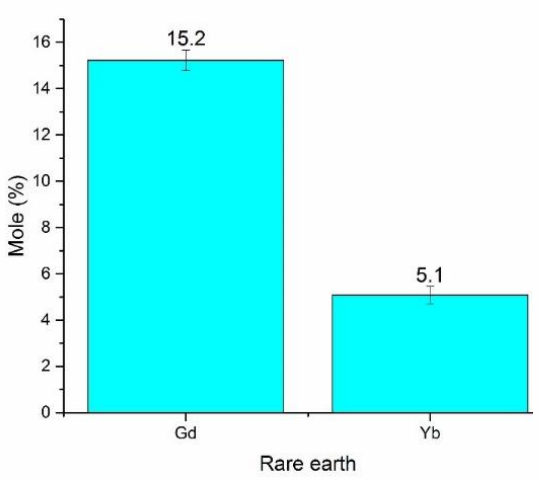

ZrO_2-9.6Y_2O_3-2.2Gd_2O_3-2.1Yb_2O_3

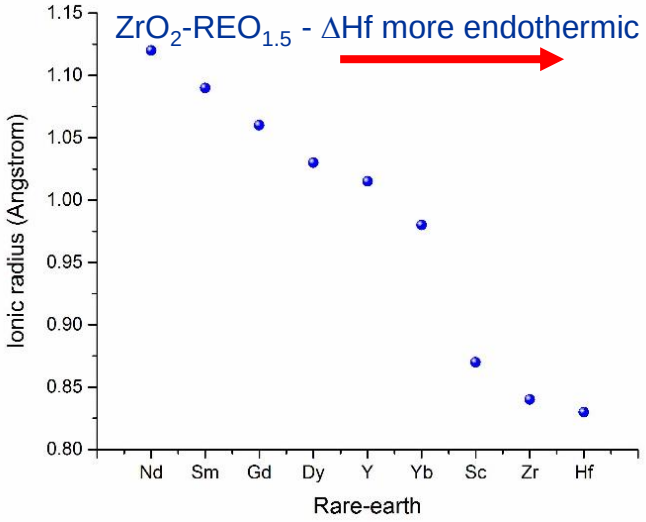

Radius size trend of RE

Summary

- Thermochemical reactions between CMAS and EBC and TBC materials were studied at 1310 °C for 5h.
- CMAS penetrated the samples at the grain boundaries and dissolved the EBC/TBC material to form silicate glassy and orthosilicate crystalline phases containing the rare-earth elements.
- Apatite crystalline phase was formed in the samples with rare-earth content higher than 12 mole (%) total of Rare-earths in the reaction zone.

- 7DySH, ZrO_2-9.5Y_2O_3-2.2Gd_2O_3-2.1Yb_2O_3 and 30YSZ samples had lower reactivity or more resistance to CMAS than the other coating compositions investigated in this study.

Acknowledgements

This work was supported by NASA Transformational Tools and Technologies Project, and also partially supported by the NASA-Army Research Laboratory Collaborative High Temperature Functionally Graded Sandphobic Coating and Surface Modification Research Project under NASA-Army Space Act Agreement SAA3-1460-1.